Crossed Andreev reflection at ferromagnetic domain walls

R. Mélin
Centre de Recherches sur les Très Basses Températures (CRTBT), Boîte Postale 166, 38042 Grenoble Cedex 9, France

S. Peysson
Instituut voor Theoretische Fysica, Universiteit van Amsterdam, Valckenierstraat 65, 1018XE Amsterdam, The Netherlands
(Received 12 February 2003; revised manuscript received 27 June 2003; published 11 November 2003)

We investigate several factors controlling the physics of hybrid structures involving ferromagnetic domain walls (DW's) and superconducting (*S*) metals. We discuss the role of noncollinear magnetizations in *S*/DW junctions in a spin⊗Nambu⊗Keldysh formalism. We discuss transport in *S*/DW/normal metal (*N*) and *S*/DW/*S* junctions in the presence of inelastic scattering in the domain wall. In this case transport properties are similar for the *S*/DW/*S* and *S*/DW/*N* junctions and are controlled by sequential tunneling of spatially separated Cooper pairs across the domain wall. In the absence of inelastic scattering we find that a Josephson current circulates only if the size of the ferromagnetic region is smaller than the elastic mean free path meaning that the Josephson effect associated with the crossed Andreev reflection cannot be observed under usual experimental conditions. Nevertheless, a finite dc current can circulate across the *S*/DW/*S* junction due to crossed Andreev reflection associated with sequential tunneling.

DOI: 10.1103/PhysRevB.68.174515 PACS number(s): 74.50.+r, 72.10.Bg

I. INTRODUCTION

A simple way of obtaining correlated pairs of electrons in solid-state devices is to extract Cooper pairs from a BCS superconductor. Devices based on this principle have focused on an important interest recently. For instance, entangled pairs of electrons can be manipulated in double-dot experiments.[1] Other devices involving a larger number of quantum dots have been proposed recently as a quantum teleportation experiment.[2] Devices involving several ferromagnetic electrodes connected to a superconductor have been investigated recently.[3–6] Noise correlations can also provide useful information about quantum entanglement.[7]

Many phenomena are involved in the proximity effect at ferromagnet/superconductor (F/S) interfaces. For instance, it is well established that the pair amplitude induced in a ferromagnetic metal oscillates in space. An interesting consequence is the possibility of fabricating $S/F/S$ π junctions in which the Josephson relation is $I=I_c \sin(\varphi+\pi)$.[8–15] In $F/S/F$ trilayers the superconducting transition temperature is larger that in the antiferromagnetic alignment of the ferromagnetic electrodes[16,17] because a finite exchange field is induced in the superconductor in the ferromagnetic alignment. On the other hand there exist ''nonlocal'' superconducting correlations coupling the two ferromagnetic electrodes that favor $\Delta_F > \Delta_{\mathrm{AF}}$ (the zero-temperature superconducting order parameter is larger in the ferromagnetic alignment).[18,19] It is also well known that the superconducting transition temperature of F/S multilayers oscillates as the thickness of the ferromagnetic layers is increased.[20–25] Several recent works have investigated new phenomena taking place in diffusive F/S heterostructures.[26–31] Other recent works were devoted to understand the interplay between the Andreev reflection and spin polarization at a single F/S interface.[32–34]

In a recent article Giroud *et al.* have proposed on the basis of experiments that the proximity effect at F/S interfaces could be strongly modified by the presence of Cooper-pair-like states propagating along domain walls (DW's).[31] These Cooper-pair-like states correspond to pair states in which the spin-up and spin-down electrons propagate in a neighboring spin-up and spin-down magnetic domain. This proximity effect is not strictly speaking equivalent to the proximity effect a normal metal $(N)/S$ interfaces. The reason is that the pair correlations induced in the N side of a N/S interface have entangled orbital and spin degrees of freedom.[7] By contrast for half-metal ferromagnets the wave function associated with the propagation of superconducting correlations along domain walls is given by the product state $|e,\alpha,\uparrow\rangle \otimes |e,\beta,\downarrow\rangle$, where α and β represent two points in neighboring magnetic domains. Another difference between a N/S interface and a multiterminal hybrid structure is that the incoming electron and the Andreev reflected hole propagate in different electrodes in multiterminal structures. As a consequence the Andreev reflected hole cannot follow the same trajectory as the incoming electron. This has important consequences regarding disorder averaging.

The purpose of our article is to investigate theoretically the mechanisms by which the Cooper-pair-like state $|e,\alpha,\uparrow\rangle\otimes|e,\beta,\downarrow\rangle$ can propagate along a ferromagnetic domain wall and to investigate several new situations that may be the object of experiments in the future. In Sec. III we discuss the perturbative transport formula of a *S*/DW junction in which the domain wall consists of many independent channels in parallel having a rotating magnetization. To discuss this model we use the spin⊗Nambu⊗Keldysh formalism described in Sec. II. For the sake of obtaining analytical results we restrict the discussion to the transport formula obtained within lowest-order perturbation theory.

If propagation in the ferromagnet is phase coherent, then the pair state $|e,\alpha,\uparrow\rangle\otimes|e,\beta,\downarrow\rangle$ injected at one end of the domain wall can propagate to the other end. On the other hand, if the phase coherence length l_ϕ is small compared to the size of the ferromagnetic region, then inelastic scattering

processes are strong and there are just a spin-up and a spin-down electron propagating independently in the spin-up and spin-down magnetic domains. There is no Josephson current but there exists a crossed Andreev reflection taking place locally at each F/S interface, so that the conductance is larger in the presence of the domain wall.

In Sec. IV we discuss the S/DW/N and S/DW/S junctions in a regime where transport properties are dominated by inelastic scattering in the domain wall. The domain wall is represented by two channels in parallel, with an opposite magnetization. This schematic model of the domain wall is expected to capture the essential physics and can be a useful comparison for more realistic studies involving numerical simulations that we plan to carry out in the future. We show that within the lowest-order perturbation the transport properties are governed by processes taking place locally at each interface once the summation over the different conduction channels has been carried out. The chemical potentials in the domain wall are determined by evaluating the current circulating through each interface and imposing current conservation.

In Sec. V we consider the other situation where inelastic scattering within the domain wall can be neglected. In this situation a finite average Josephson current can circulate between the two superconductors of the S/DW/S junction only if the size of the ferromagnetic region is smaller than the elastic mean free path. This condition is not realized with usual ferromagnets and we come to the conclusion that there is no Josephson current under usual experimental conditions. Final remarks are given in Sec. VI.

To conclude the introductory section we note that the theory of inhomogeneous ferromagnets with noncollinear magnetizations in contact with a superconductor was already elaborated in Refs. 35 and 36 in connection with the long-range proximity effect associated with the triplet component of the superconducting condensate. In our article the emphasis is put on other aspects of this problem (the transport of spatially separated Cooper pairs). Both effects may play a relevant role in experiments. Finally a recent work[37] appeared in which the conductance of a S/DW junction was calculated independently of our work.

II. PRELIMINARIES

A. Spin⊗Nambu⊗Keldysh formalism

The direction of the magnetization is rotating in a ferromagnetic domain wall. To describe superconducting correlations in the presence of noncollinear magnetizations we use a spin⊗Nambu⊗Keldysh formalism.[38–40] The advanced Green's function is a 4×4 matrix:

$$\hat{G}^A_{i,j}(t,t') = -i\,\theta(t-t') \begin{bmatrix} \langle\{c^\dagger_{j,\uparrow}(t'),c_{i,\uparrow}(t)\}\rangle & \langle\{c_{j,\downarrow}(t'),c_{i,\uparrow}(t)\}\rangle & \langle\{c^\dagger_{j,\downarrow}(t'),c_{i,\uparrow}(t)\}\rangle & \langle\{c_{j,\uparrow}(t'),c_{i,\uparrow}(t)\}\rangle \\ \langle\{c^\dagger_{j,\uparrow}(t'),c^\dagger_{i,\downarrow}(t)\}\rangle & \langle\{c_{j,\downarrow}(t'),c^\dagger_{i,\downarrow}(t)\}\rangle & \langle\{c^\dagger_{j,\downarrow}(t'),c^\dagger_{i,\downarrow}(t)\}\rangle & \langle\{c_{j,\uparrow}(t'),c^\dagger_{i,\downarrow}(t)\}\rangle \\ \langle\{c^\dagger_{j,\uparrow}(t'),c_{i,\downarrow}(t)\}\rangle & \langle\{c_{j,\downarrow}(t'),c_{i,\downarrow}(t)\}\rangle & \langle\{c^\dagger_{j,\downarrow}(t'),c_{i,\downarrow}(t)\}\rangle & \langle\{c_{j,\uparrow}(t'),c_{i,\downarrow}(t)\}\rangle \\ \langle\{c^\dagger_{j,\uparrow}(t'),c^\dagger_{i,\uparrow}(t)\}\rangle & \langle\{c_{j,\downarrow}(t'),c^\dagger_{i,\uparrow}(t)\}\rangle & \langle\{c^\dagger_{j,\downarrow}(t'),c^\dagger_{i,\uparrow}\}\rangle & \langle\{c_{j,\uparrow}(t'),c^\dagger_{i,\uparrow}(t)\}\rangle \end{bmatrix}. \quad (1)$$

The Dyson equation relates the Green's functions of the connected system to the Green's functions of the disconnected system. In compact notation the Dyson equation takes the form $\hat{G}=\hat{g}+\hat{g}\otimes\hat{\Sigma}\otimes\hat{G}$, where the symbol⊗includes a summation over the sites of the network and a convolution over time variables. Since we consider stationary transport the convolution over time variables becomes a simple product after a Fourier transform is carried out. The Dyson equation for the Keldysh Green's function $\hat{G}^{+,-}$ is given by[49–51]

$$\hat{G}^{+,-}=[\hat{I}+\hat{G}^R\otimes\hat{\Sigma}]\otimes\hat{g}^{+,-}\otimes[\hat{I}+\hat{\Sigma}\otimes\hat{G}^A], \quad (2)$$

where the self-energy $\hat{\Sigma}$ contains all the couplings present in the tunnel Hamiltonian. The tunnel Hamiltonian corresponding to Fig. 1 takes the form

$$\mathcal{W}=\sum_\sigma [t_{a,\alpha}c^\dagger_{a,\sigma}c_{\alpha,\sigma}+t_{\alpha,a}c^\dagger_{\alpha,\sigma}c_{a,\sigma}+t_{b,\beta}c^\dagger_{b,\sigma}c_{\beta,\sigma} + t_{\beta,b}c^\dagger_{\beta,\sigma}c_{b,\sigma}]. \quad (3)$$

The current through the link a-α is given by

$$I_{a,\alpha}=\frac{e}{2h}\int \mathrm{Tr}\{\hat{\sigma}_z[\hat{t}_{a,\alpha}\hat{G}^{+,-}_{\alpha,a}-\hat{t}_{\alpha,a}\hat{G}^{+,-}_{a,\alpha}]\}d\omega, \quad (4)$$

where the matrix $\hat{\sigma}_z$ is given by

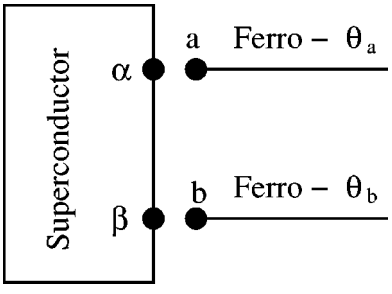

FIG. 1. The device involving crossed Andreev reflection and elastic cotunneling with noncollinear magnetizations. Electrode ending at site "a" is a ferromagnet with a magnetization pointing in the direction θ_a. Electrode ending at site "b" is a ferromagnet with a magnetization pointing in the direction θ_b.

$$\hat{\sigma}_z = \begin{bmatrix} 1 & 0 & 0 & 0 \\ 0 & -1 & 0 & 0 \\ 0 & 0 & 1 & 0 \\ 0 & 0 & 0 & -1 \end{bmatrix} \tag{5}$$

and the Nambu representation of the hopping matrix elements is given by $\hat{t}_{a,\alpha}=t_{a,\alpha}\hat{\sigma}_z$, $\hat{t}_{\alpha,a}=t_{\alpha,a}\hat{\sigma}_z$, $\hat{t}_{b,\beta}=t_{b,\beta}\hat{\sigma}_z$, $\hat{t}_{\beta,b}=t_{\beta,b}\hat{\sigma}_z$.

B. Green's function of a ferromagnetic metal

Now we give the expressions of the Green's functions of a ferromagnetic metal. We first suppose that the spin quantization axis is parallel to the direction of the magnetization. The Green's function takes the form

$$\hat{g}(R,\omega) = \begin{bmatrix} g_{1,1}(R,\omega) & 0 & 0 & 0 \\ 0 & g_{2,2}(R,\omega) & 0 & 0 \\ 0 & 0 & g_{3,3}(R,\omega) & 0 \\ 0 & 0 & 0 & g_{4,4}(R,\omega) \end{bmatrix}. \tag{6}$$

The four diagonal elements are given by

$$g_{1,1}(R,\omega) = -\frac{m_\uparrow a_0^2}{\hbar^2}\frac{a_0}{2\pi R}\exp\left\{-i\left(k_F^\uparrow + \frac{\omega}{v_F^\uparrow}\right)R\right\} \times \exp\left\{-\left(\frac{R}{l_\phi}\right)\right\}, \tag{7}$$

$$g_{2,2}(R,\omega) = \frac{m_\downarrow a_0^2}{\hbar^2}\frac{a_0}{2\pi R}\exp\left\{i\left(k_F^\downarrow - \frac{\omega}{v_F^\downarrow}\right)R\right\}\exp\left\{-\left(\frac{R}{l_\phi}\right)\right\}, \tag{8}$$

$$g_{3,3}(R,\omega) = -\frac{m_\downarrow a_0^2}{\hbar^2}\frac{a_0}{2\pi R}\exp\left\{-i\left(k_F^\downarrow + \frac{\omega}{v_F^\downarrow}\right)R\right\} \times \exp\left\{-\left(\frac{R}{l_\phi}\right)\right\}, \tag{9}$$

$$g_{4,4}(R,\omega) = \frac{m_\uparrow a_0^2}{\hbar^2}\frac{a_0}{2\pi R}\exp\left\{i\left(k_F^\uparrow - \frac{\omega}{v_F^\uparrow}\right)R\right\} \times \exp\left\{-\left(\frac{R}{l_\phi}\right)\right\}, \tag{10}$$

where we have introduced a Fermi wave-vector mismatch as well as a mismatch between the spin-up and spin-down Fermi velocities. The parameter a_0 is equal to the distance between neighboring sites on the cubic lattice. For generality we introduced a different mass for the spin-up and spin-down electrons, meaning that the spin-up density of states is different from the spin-down density of states. The local propagators are defined by

$$g_{1,1}^{\mathrm{loc}} = g_{4,4}^{\mathrm{loc}} = i\frac{a_0 k_F^\uparrow}{2\pi}\frac{m_\uparrow a_0^2}{\hbar^2} = i\pi\rho_F\left(\frac{1+P}{2}\right), \tag{11}$$

$$g_{2,2}^{\mathrm{loc}} = g_{3,3}^{\mathrm{loc}} = i\frac{a_0 k_F^\downarrow}{2\pi}\frac{m_\downarrow a_0^2}{\hbar^2} = i\pi\rho_F\left(\frac{1-P}{2}\right). \tag{12}$$

We also introduced phenomenologically in Eqs. (7)–(10) an exponential decay of the correlations due to the presence of a finite coherence length l_ϕ in the ferromagnet. l_ϕ is usually smaller than the dimension of the ferromagnetic metal. In this case ferromagnetism can be treated semiclassically as in the theoretical description of the giant magnetoresistance.[41–43] However, Aharonov-Bohm oscillations in a ferromagnetic nanoring have been reported recently.[44] The inner diameter of the Fe-Ni nanoring in Ref. 44 is 420 Å and the outer diameter is 500 Å.

We will use in Sec. III the expression of the local Green's functions of a ferromagnetic metal with the quantization axis not parallel to the magnetization. We suppose that the direction of the exchange field is rotated by an angle θ around the x axis. We do not incorporate a rotation of angle φ around the z axis since this rotation just introduces simple phase factors. The local Green's function of the rotated ferromagnet takes the form

$$\hat{g}_{\mathrm{loc}} = i\pi\tilde{\rho}\begin{bmatrix} 1+P\cos\theta & 0 & -iP\sin\theta & 0 \\ 0 & 1-P\cos\theta & 0 & -iP\sin\theta \\ iP\sin\theta & 0 & 1-P\cos\theta & 0 \\ 0 & iP\sin\theta & 0 & 1+P\cos\theta \end{bmatrix}, \tag{13}$$

where $\tilde{\rho}=(\rho_\uparrow+\rho_\downarrow)/2$ is the average density of states at the Fermi level and $P=(\rho_\uparrow-\rho_\downarrow)/(\rho_\uparrow+\rho_\downarrow)$ is the spin polarization at the Fermi level.

We will also use in Sec. V B the expression of the full propagator $\hat{g}(R,\omega)$ of a rotated ferromagnet. The Green's function takes the form

$$\hat{g}(R,\omega)=\begin{bmatrix} \tilde{g}_{1,1} & O & \tilde{g}_{1,3} & 0 \\ 0 & \tilde{g}_{2,2} & 0 & \overline{g}_{2,4} \\ \tilde{g}_{3,1} & O & \tilde{g}_{3,3} & 0 \\ 0 & \tilde{g}_{4,2} & 0 & \tilde{g}_{4,4} \end{bmatrix}, \tag{14}$$

where the diagonal elements are given by

$$\tilde{g}_{1,1}=\tfrac{1}{2}(g_{1,1}+g_{3,3})+\tfrac{1}{2}\cos\theta(g_{1,1}-g_{3,3}), \tag{15}$$

$$\tilde{g}_{2,2}=\tfrac{1}{2}(g_{2,2}+g_{4,4})+\tfrac{1}{2}\cos\theta(g_{2,2}-g_{4,4}), \tag{16}$$

$$\tilde{g}_{3,3}=\tfrac{1}{2}(g_{3,3}+g_{1,1})+\tfrac{1}{2}\cos\theta(g_{3,3}-g_{1,1}), \tag{17}$$

$$\tilde{g}_{4,4}=\tfrac{1}{2}(g_{4,4}+g_{2,2})+\tfrac{1}{2}\cos\theta(g_{4,4}-g_{2,2}), \tag{18}$$

where $g_{1,1}$, $g_{2,2}$, $g_{3,3}$, and $g_{4,4}$ are given by Eqs. (7)–(10). The extradiagonal elements are given by

$$\tilde{g}_{1,3}=-\tilde{g}_{3,1}=\frac{i}{2}\sin\theta(g_{3,3}-g_{1,1}), \tag{19}$$

$$\tilde{g}_{2,4}=-\tilde{g}_{4,2}=\frac{i}{2}\sin\theta(g_{2,2}-g_{4,4}). \tag{20}$$

C. 4×4 Green's functions of a superconductor

The Green's function of a superconductor takes the form

$$\hat{g}^{A,R}(R,\omega)=\begin{bmatrix} g(R,\omega) & f(R,\omega) & 0 & 0 \\ f(R,\omega) & g'(R,\omega) & 0 & 0 \\ 0 & 0 & g(R,\omega) & -f(R,\omega) \\ 0 & 0 & -f(R,\omega) & g'(R,\omega) \end{bmatrix}. \tag{21}$$

The matrix elements of the Green's function are given by

$$g(R,\omega)=\frac{ma_0^2}{\hbar^2}\frac{a_0}{2\pi R}\exp\left(-\frac{R}{\xi(\omega)}\right)\times\left\{\sin(k_FR)\frac{-\omega}{\sqrt{\Delta^2-\omega^2}}-\cos(k_FR)\right\}, \tag{22}$$

$$g'(R,\omega)=\frac{ma_0^2}{\hbar^2}\frac{a_0}{2\pi R}\exp\left(-\frac{R}{\xi(\omega)}\right)\times\left\{\sin(k_FR)\frac{-\omega}{\sqrt{\Delta^2-\omega^2}}+\cos(k_FR)\right\}, \tag{23}$$

$$f(R,\omega)=\frac{ma_0^2}{\hbar^2}\frac{a_0}{2\pi R}\exp\left(-\frac{R}{\xi(\omega)}\right)\sin(k_FR)\frac{\Delta}{\sqrt{\Delta^2-\omega^2}}, \tag{24}$$

where we supposed that $\omega<\Delta$. The coherence length is given by $\xi(\omega)=\hbar v_F/\sqrt{\Delta^2-\omega^2}$.

D. 4×4 Green's functions of a superconductor in a uniform magnetic field

A uniform magnetic field h_S can penetrate in a superconductor if the superconductor is in a thin-film geometry[45] and the magnetic field is parallel to the direction of the superconducting film. The effect of the magnetic field is a Zeeman splitting of the spin-up and spin-down quasiparticle bands. Let us suppose that the quantization axis is parallel to the orientation of the magnetic field. The 4×4 Green's function takes the form

$$g^{A,R}(R,\omega)=\begin{bmatrix} g_+(R,\omega) & f_+(R,\omega) & 0 & 0 \\ f_+(R,\omega) & g'_+(R,\omega) & 0 & 0 \\ 0 & 0 & g_-(R,\omega) & -f_-(R,\omega) \\ 0 & 0 & -f_-(R,\omega) & g'_-(R,\omega) \end{bmatrix}, \tag{25}$$

with $g_+(R,\omega)=g(R,\omega+h_S)$, $g'_+(R,\omega)=g'(R,\omega+h_S)$, $f_+(R,\omega)=f(R,\omega+h_S)$, $g_-(R,\omega)=g(R,\omega-h_S)$, $g'_-(R,\omega)=g'(R,\omega-h_S)$, and $f_-(R,\omega)=f(R,\omega-h_S)$.

III. CROSSED ANDREEV REFLECTION AND ELASTIC COTUNNELING WITH NONCOLLINEAR MAGNETIZATIONS

A. Transport formula

In this section we evaluate the transport formula corresponding to the device on Fig. 1 in which the magnetization of electrode a (b) makes an angle θ_a (θ_b) with the z axis. Using the formalism described in Sec. II we obtain the current per conduction channel through electrode a to lowest order in $t_{a,\alpha}$ and $t_{b,\beta}$:

$$I_{a,\alpha}=\frac{e}{h}\int d\omega\, 8\pi^2t_\alpha^4\tilde{\rho}_a^2(1-P_a^2)f_{\rm loc}^2(\omega)[n_F(\omega-eV_a)-n_F(\omega+eV_a)]+\frac{e}{h}\int d\omega\, 4\pi^2t_\alpha^2t_\beta^2\tilde{\rho}_a\tilde{\rho}_b[1+P_aP_b\cos(\theta_a-\theta_b)]$$
$$\times\langle\langle g_{\alpha,\beta}g_{\beta,\alpha}\rangle\rangle[n_F(\omega-eV_a)-n_F(\omega+eV_a)-n_F(\omega-eV_b)+n_F(\omega+eV_b)]+\frac{e}{h}\int d\omega\, 4\pi^2t_\alpha^2t_\beta^2\tilde{\rho}_a\tilde{\rho}_b$$
$$\times[1-P_aP_b\cos(\theta_a-\theta_b)]\langle\langle f_{\alpha,\beta}f_{\beta,\alpha}\rangle\rangle[n_F(\omega-eV_a)-n_F(\omega+eV_a)+n_F(\omega-eV_b)-n_F(\omega+eV_b)]. \tag{26}$$

We have assumed that electrodes *a* and *b* are made of a large number of independent conduction channels in parallel so that we make an averaging over the microscopic phases in the propagators. Now if we consider that the same voltage is applied on both electrodes the conductance is given by the local Andreev reflection and crossed Andreev reflection:

$$G=32\pi^2\frac{e^2}{h}t_\alpha^4\tilde{\rho}_a^2(1-P_a^2)f_{\rm loc}^2+32\pi^2\frac{e^2}{h}t_\alpha^2t_\beta^2\tilde{\rho}_a\tilde{\rho}_b \times[1-P_aP_b\cos(\theta_a-\theta_b)]\langle\langle f_{\alpha,\beta}f_{\beta,\alpha}\rangle\rangle. \quad (27)$$

B. Conductance associated to a domain wall

Let us now consider the situation in Fig. 2 representing a *S*/DW contact between a superconductor and a magnetic domain wall. We suppose that the ferromagnetic metal is made of a collection of independent channels. The magnetization is rotating inside the domain wall, meaning that the angle θ is a function of *z*: $\theta=\theta(z)$. We want to evaluate the difference $G^{(\rm DW)}-G^{(0)}$ between the conductances $G^{(\rm DW)}$ in the presence of the domain wall and $G^{(0)}$ in the absence of the domain wall. To obtain the conductance we sum the contributions of the different channels (see Fig. 2) and we obtain

$$G^{(\rm DW)}-G^{(0)}=4\frac{e^2}{h}\frac{L_y}{a_0}t^4\overline{\rho}^2P^2\left(\frac{ma_0^2}{\hbar^2}\right)^2F(\xi_0,D), \quad (28)$$

with

$$F(\xi_0,D)=\int\frac{d(\Delta y)}{a_0}\int\frac{dz_a}{a_0}\int\frac{dz_b}{a_0}\frac{a_0^2}{(\Delta y)^2+(z_a-z_b)^2} \times\sin^2\left(\frac{\theta(z_a)-\theta(z_b)}{2}\right) \times\exp\left(-\frac{2\sqrt{(\Delta y)^2+(z_a-z_b)^2}}{\xi_0}\right), \quad (29)$$

where $\xi_0=\hbar v_F/\Delta$ is the BCS coherence length at zero energy and *D* is the width of the domain wall. L_y is equal to the dimension of the junction in the *y* direction and we used the notation $\Delta y=y_a-y_b$. To obtain Eq. (29) we have supposed that the width of the domain wall is much larger than the Fermi wavelength so that we can average over the microscopic phase variables in the propagator $f_{\alpha,\beta}$ [see Eq. (24)].

The crossed Andreev reflection cannot take place between the channels separated by a distance much smaller than the width *D* of the domain wall because such channels have an almost parallel magnetization. The crossed Andreev reflection cannot take place either between channels separated by a distance much larger than the superconducting coherence length because of the exponential decay of the propagator $f_{\alpha,\beta}$. As a consequence the value of $G^{(\rm DW)}-G^{(0)}$ is the largest if the width of the domain wall is small compared to the BCS coherence length. This is illustrated in Fig. 3 where we have represented the variation of the conductance as a function of ξ_0 for different values of *D* and for the domain wall profile given by

$$\theta(z)=\arctan(z/D). \quad (30)$$

C. Exchange field in the superconductor due to the proximity effect

Now we come back to a system in which two ferromagnetic electrodes are connected to a superconductor. An exchange field can be generated in the superconductor because of the proximity effect. This was first observed in Ref. 16 in the case of insulating ferromagnets. An exchange field in a superconductor is a pair-breaking perturbation. As a consequence in the *F*/*S*/*F* trilayer with insulating ferromagnets the order parameter is larger in the antiferromagnetic alignment of the ferromagnetic electrodes.[16] This was well verified in experiments with insulating ferromagnets.[46,47] The same effect is present with metallic ferromagnets[17,19] but in this case there exists also pair correlations induced in the ferromagnetic electrodes[18,19] that can modify the value of the self-consistent order parameter.

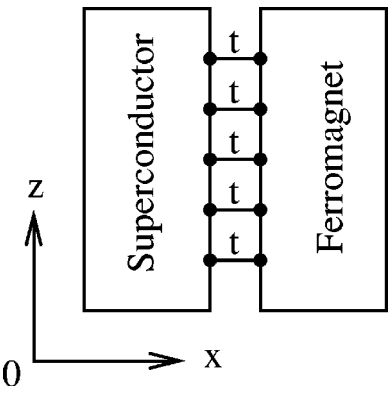

FIG. 2. The device involving a *S*/DW junction between a superconductor and a ferromagnetic domain wall. In the ferromagnet the local magnetization makes an angle $\theta(z)$ with the *z* axis. The *x* and *z* axes are in the plane of the figure. The *y* axis is perpendicular to the plane of the figure.

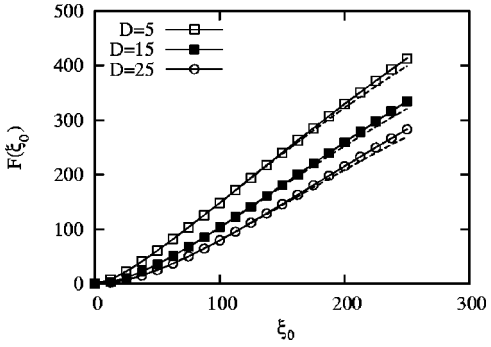

FIG. 3. Variation of $F(\xi_0,D)$ as a function of ξ_0 for different values of *D*. We used the domain wall profile given by Eq. (30) in a three-dimensional geometry. The distance between neighboring channels is $a_0=1$. We introduced a cutoff $-L_y/2\leqslant\Delta y\leqslant L_y$, $-L_z/2\leqslant z_a$, $z_b\leqslant L_z/2$ in the expression of $F(\xi_0,D)$ [see Eq. (29)]. The solid lines correspond to $L_y=L_z=500$ and the dashed line (almost superimposed with the solid line) corresponds to $L_y=L_z=600$.

We suppose that the magnetizations in electrodes a and b make an angle θ_a and θ_b and that an exchange field h_S is induced in the superconductor. Without loss of generality we suppose that the direction of the exchange field in the superconductor is parallel to the quantization axis. In terms of the g_+, f_+, g_-, and f_- introduced in Sec. II D the transport formula is found to be

$$I_{a,\alpha}=\frac{e}{h}\int d\omega\, 4\pi^2 t_\alpha^4 \tilde{\rho}_a^2[(f_+^2+f_-^2)(1-P_a^2\cos^2\theta_a) - 2\, f_+ f_- P_a^2 \sin^2\theta_a][n_F(\omega-eV_a)-n_F(\omega+eV_a)] \tag{31}$$

$$+\frac{e}{h}\int d\omega\, 2\pi^2 t_\alpha^2 t_\beta^2 \tilde{\rho}_a\tilde{\rho}_b\{[\langle\langle g^+_{\alpha,\beta}g^+_{\beta,\alpha}\rangle\rangle + \langle\langle g^-_{\alpha,\beta}g^-_{\beta,\alpha}\rangle\rangle][1+P_aP_b\cos\theta_a\cos\theta_b] + 2\langle\langle g^+_{\alpha,\beta}g^-_{\beta,\alpha}\rangle\rangle P_aP_b\sin\theta_a\sin\theta_b\}[n_F(\omega-eV_a) - n_F(\omega+eV_a)-n_F(\omega-eV_b)+n_F(\omega+eV_b)] \tag{32}$$

$$+\frac{e}{h}\int d\omega\, 2\pi^2 t_\alpha^2 t_\beta^2 \tilde{\rho}_a\tilde{\rho}_b\{[\langle\langle f^+_{\alpha,\beta}f^+_{\beta,\alpha}\rangle\rangle + \langle\langle f^-_{\alpha,\beta}f^-_{\beta,\alpha}\rangle\rangle]\times[1-P_aP_b\cos\theta_a\cos\theta_b] - 2\langle\langle f^+_{\alpha,\beta}f^-_{\beta,\alpha}\rangle\rangle P_aP_b\sin\theta_a\sin\theta_b\}[n_F(\omega-eV_a) - n_F(\omega+eV_a)+n_F(\omega-eV_b)-n_F(\omega+eV_b)]. \tag{33}$$

The term (31) corresponds to the local Andreev reflection. The term (32) corresponds to elastic cotunneling and the term (33) corresponds to the crossed Andreev reflection. The term $\langle\langle g^+_{\alpha,\beta}g^+_{\beta,\alpha}\rangle\rangle$ corresponds to a process in which a spin-up electron travels from electrode a to electrode b and comes back to electrode a as a spin-up electron. The term $\langle\langle g^+_{\alpha,\beta}g^-_{\beta,\alpha}\rangle\rangle$ corresponds to a process in which a spin-up electron travels from electrode a to electrode b, undergoes a spin precession in electrode b, and comes back as a spin-down electron traveling from electrode b to electrode a.

Replacing the propagators involved in Eqs. (31)–(33) by their expressions given in Sec. II C leads to the transport formula to lowest order in h_S and ω:

$$I_{a,\alpha}=8\pi^2 t_\alpha^4\left(\frac{ma_0^2}{\hbar^2}\right)^2\left(\frac{a_0}{2\pi R_0}\right)^2\left[1+\frac{\omega^2+h_S^2}{\Delta^2}\right][1-P_a^2]\times[n_F(\omega-eV_a)-n_F(\omega+eV_a)] \tag{34}$$

$$+2\pi^2 t_\alpha^2 t_\beta^2\tilde{\rho}_a\tilde{\rho}_b\left(\frac{ma_0^2}{\hbar^2}\right)^2\left(\frac{a_0}{2\pi R_{\alpha,\beta}}\right)^2\exp\left(-\frac{2R_{\alpha,\beta}}{\xi(\omega)}\right)\times\left\{1+\left[1+\frac{\omega^2}{\Delta^2}\right]P_aP_b\cos(\theta_a-\theta_b)+\frac{h_S^2}{\Delta^2}P_aP_b\times\cos(\theta_a+\theta_b)\right\}[n_F(\omega-eV_a)-n_F(\omega+eV_a) - n_F(\omega-eV_b)+n_F(\omega+eV_b)] \tag{35}$$

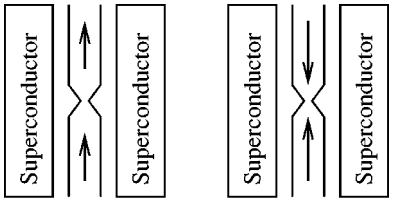

FIG. 4. The device considered in Sec. IV. In (a) there is no domain wall in the junction. In (b) a domain wall is pinned in the junction.

$$+2\pi^2 t_\alpha^2 t_\beta^2\tilde{\rho}_a\tilde{\rho}_b\left(\frac{ma_0^2}{\hbar^2}\right)\left(\frac{a_0}{2\pi R_{\alpha,\beta}}\right)^2\exp\left(-\frac{2R_{\alpha,\beta}}{\xi(\omega)}\right)\times\left[1+\frac{\omega^2+h_S^2}{\Delta^2}\right][1-P_aP_b\cos(\theta_a-\theta_b)][n_F(\omega-eV_a) - n_F(\omega+eV_a)+n_F(\omega-eV_b)-n_F(\omega+eV_b)], \tag{36}$$

where $k_FR_0=\pi/2$ is the ultraviolet cutoff used to define the local propagator involved in the local Andreev reflection. We see that the crossed Andreev reflection term given by term (35) is not identical to the elastic cotunneling term given by term (36). This shows that the symmetry between elastic cotunneling and the crossed Andreev reflection is broken by the exchange field in the superconductor. This can be illustrated by considering that electrode b is a normal metal: $P_b=0$. The crossed conductance at zero voltage is finite if the exchange field h_S in the superconductor takes a finite value:

$$G_{a,b}=\frac{\partial I_a}{\partial V_b}=4\pi^2 t_\alpha^2 t_\beta^2\tilde{\rho}_a\tilde{\rho}_b\left(\frac{ma_0^2}{\hbar^2}\right)^2\left(\frac{a_0}{2\pi R_{\alpha,\beta}}\right)^2\times\exp\left(-\frac{2R_{\alpha,\beta}}{\xi_0}\right)\left(\frac{h_S}{\Delta}\right)^2. \tag{37}$$

By comparison we have $G_{a,b}=0$ if $h_S=0$ because of a cancellation between the crossed Andreev reflection and elastic cotunneling conductances. We thus see that a crossed Andreev reflection experiment with a ferromagnetic and a normal-metal electrode can give information about the existence of an induced exchange field in the superconductor. We see also from Eqs. (31)–(33) that there is no precession of the electron spin around the direction of the exchange field in the superconductor. The absence of spin precession in the superconducting case can be contrasted with the metallic case (see Appendix A).

IV. SEQUENTIAL TUNNELING OF COOPER PAIRS THROUGH A MAGNETIC DOMAIN WALL

Now we consider the junction on Fig. 4 in which a ferromagnetic wire is inserted between two superconductors. In the absence of a domain wall in the ferromagnetic wire [see Fig. 4(a)] the junction is just a $S/F/S$ junction. In the presence of a domain wall [see Fig. 4(b)] Cooper-pair-like states arising from a crossed Andreev reflection can be transmitted through the junction. As a consequence the conductance is

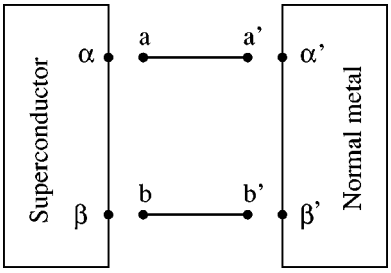

FIG. 5. The device considered in Sec. IV C in which two single-channel electrodes representing two magnetic domains are inserted in between a superconductor and a normal metal. The two electrodes ending at sites a and a' and sites b and b' are ferromagnetic. In Secs. IV D and V we suppose that the electrode containing the sites α' and β' is superconducting.

larger in the presence of a magnetic domain wall. We consider two limiting cases:

(i) Transport is dominated by inelastic scattering in the ferromagnetic domains. Because of inelastic scattering the distribution functions in the ferromagnetic domains relax to the Fermi distribution. This case is discussed in Secs. IV B, IV C, and IV D.

(ii) Transport through the domain wall is phase coherent and there is a Josephson current circulating between the two ferromagnetic electrodes. This case is discussed in Sec. V.

A. The different time scales

Similarly to Ref. 48 we notice that three time scales are involved in out-of-equilibrium transport through a ferromagnetic domain wall:

(i) The transport dwell time τ_d, being the time taken by an electron to travel through one of the magnetic domains.

(ii) The energy relaxation time τ_E. Because of inelastic scattering the distribution function in the out-of-equilibrium conductor relaxes to the Fermi distribution. This relaxation takes place on a time scale τ_E.

(iii) The spin-flip time τ_{sf}, being the time above which spin-flip scattering is relevant.

We suppose in this section that $\tau_E \ll \tau_d \ll \tau_{sf}$. The distribution function in the intermediate magnetic domains is thus well approximated by a Fermi distribution. The chemical potential of spin-up electrons is different from the chemical potential of spin-down electrons.[49–51]

B. Perturbative transport formula

In this section we discuss the perturbative transport formula of the S/DW/N junction on Fig. 5. The full transport formula to order t^4 is evaluated in Appendix B. The expression of $I^{(\uparrow)}_{a,\alpha}$ contains two kinds of terms: the terms (B1)–(B3) describe processes taking place locally at the interfaces between the superconductor and the ferromagnetic electrodes without propagation in the ferromagnetic electrodes. The terms (B4)–(B7) involve propagation in the ferromagnetic electrodes. The two kinds of terms would contribute if electrodes (a,a') and (b,b') were single-channel electrodes. We consider here that electrodes (a,a') and (b,b') are multi-channel electrodes and we average the current over the microscopic phases. Once this averaging is done, only the ''local'' terms survive in the transport formula given by

$$I^{(\uparrow)}_{a,\alpha} = -4\pi^2 t_\alpha^4 \tilde{\rho}_a^2 f_{\rm loc}^2 [1-P_a^2][n_F(\omega-\mu_{a,\uparrow}) - n_F(\omega+\mu_{a,\downarrow})] \tag{38}$$

$$-4\pi^2 t_\alpha^2 t_\beta^2 \tilde{\rho}_a \tilde{\rho}_b \langle\langle g^2_{\alpha,\beta}\rangle\rangle [1+P_a][1+P_b] \times [n_F(\omega-\mu_{a,\uparrow}) - n_F(\omega-\mu_{b,\uparrow})] \tag{39}$$

$$-4\pi^2 t_\alpha^2 t_\beta^2 \tilde{\rho}_a \tilde{\rho}_b \langle\langle f^2_{\alpha,\beta}\rangle\rangle [1+P_a][1-P_b] \times [n_F(\omega-\mu_{a,\uparrow}) - n_F(\omega+\mu_{b,\downarrow})]. \tag{40}$$

The term (38) corresponds to the local Andreev reflection at the interface a-α. The term (39) corresponds to elastic cotunneling through the superconductor and the term (40) corresponds to the crossed Andreev reflection.

A similar calculation can be carried out at interface (a',α'). Once the average over the microscopic phase variables is carried out we find

$$I^{(\uparrow)}_{a',\alpha'} = -4\pi^2 t^2_{\alpha'} \tilde{\rho}_a \rho' [1+P_a][n_F(\omega-\mu_{a,\uparrow}) - n_F(\omega-\mu')] \tag{41}$$

$$+8\pi^4 t^4_{\alpha'} (\tilde{\rho}_a)^2 (\rho')^2 [1+P_a]^2 \times [n_F(\omega-\mu_{a,\uparrow}) - n_F(\omega-\mu')] \tag{42}$$

$$+8\pi^4 t^2_{\alpha'} t^2_{\beta'} \overline{\rho}_a \overline{\rho}_b \langle\langle \rho^2_{\alpha',\beta'}\rangle\rangle [1+P_a][1+P_b] \times [n_F(\omega-\mu_{b,\uparrow}) - n_F(\omega-\mu')], \tag{43}$$

where terms (41) and (42) describe electron tunneling from the electrode (a,a') into the normal metal and term (43) describes elastic cotunneling from electrode (b,b') to electrode (a,a').

C. Sequential tunneling through the S/DW/N junction

In this section we discuss out-of-equilibrium transport in a S/DW/N junction on the basis of the two-channel model shown on Fig. 5. We suppose that a voltage $V=0$ is applied on the superconductor and a voltage V' is applied on the normal metal. The spin-up and spin-down chemical potentials in the two magnetic domains (a,a') and (b,b') are determined in such a way that current is conserved. In general, there are four unknown chemical potentials ($\mu_{a,\uparrow}$, $\mu_{a,\downarrow}$, $\mu_{b,\uparrow}$, and $\mu_{b,\downarrow}$) that can be determined from four equations for current conservation. There exist two cases in which the 4×4 system of equations can be reduced to a 2×2 system of equations:

(i) Half-metal ferromagnets where there is only one spin population in each of the ferromagnetic electrodes (a,a') and (b,b'). This case is treated in the main body of the article.

(ii) The symmetric case where the two electrodes (a,a') and (b,b') have identical density of states and where $t_\alpha = t_\beta$ and $t_{\alpha'} = t_{\beta'}$. This case is treated in Appendix C.

Let us consider half-metal ferromagnets: $P_a=1$ and $P_b=-1$. The transport formula is found to be

$$\frac{I_{\rm tot}}{V'}=\frac{16\pi^2}{\mathcal{D}}t_\alpha^2t_\beta^2t_{\alpha'}^2t_{\beta'}^2\rho_{a,\uparrow}\rho_{b,\downarrow}(\rho')^2\langle\langle f_{\alpha,\beta}^2\rangle\rangle \times[1-2\pi^2t_{\alpha'}^2\rho_{a,\uparrow}\rho'][1-2\pi^2t_{\beta'}^2\rho_{b,\downarrow}\rho'], \quad (44)$$

with

$$\mathcal{D}=t_\alpha^2t_\beta^2t_{\alpha'}^2\rho_{a,\uparrow}\rho'\langle\langle f_{\alpha,\beta}^2\rangle\rangle[1-2\pi^2t_{\alpha'}^2\rho_{a,\uparrow}\rho'] +t_\alpha^2t_\beta^2t_{\beta'}^2\rho_{b,\downarrow}\rho'\langle\langle f_{\alpha,\beta}^2\rangle\rangle[1-2\pi^2t_{\beta'}^2\rho_{b,\downarrow}\rho'] +t_{\alpha'}^2t_{\beta'}^2(\rho')^2[1-2\pi^2t_{\alpha'}^2\rho_{a,\uparrow}\rho'][1-2\pi^2t_{\beta'}^2\rho_{b,\downarrow}\rho']. \quad (45)$$

We note ρ_N, a typical value of the density of states, either in the superconductor or in the ferromagnetic and normal-metal electrodes. We first suppose that $t_\alpha^2\rho_N$ and $t_\beta^2\rho_N$ are small compared to $t_{\alpha'}$ and $t_{\beta'}$. The transport formula takes the same form as in the case where the ferromagnetic electrodes (a,a') and (b,b') are in equilibrium:

$$\frac{I_{\rm tot}}{V'}=16\pi^2t_\alpha^2t_\beta^2\rho_{a,\uparrow}\rho_{b,\downarrow}\langle\langle f_{\alpha,\beta}^2\rangle\rangle. \quad (46)$$

In the other limiting case where $t_\alpha^2\rho_N$ and $t_\beta^2\rho_N$ are large compared to $t_{\alpha'}$ and $t_{\beta'}$ we find

$$\frac{I_{\rm tot}}{V'}=16\pi^2\rho'\frac{t_{\alpha'}^2t_{\beta'}^2\rho_{a,\uparrow}\rho_{b,\downarrow}}{t_{\alpha'}^2\rho_{a,\uparrow}+t_{\beta'}^2\rho_{b,\downarrow}}. \quad (47)$$

We note $g_a=16\pi^2t_{\alpha'}^2\rho_{a,\uparrow}\rho'$ and $g_b=16\pi^2t_{\alpha'}^2\rho_{b,\downarrow}\rho'$, the conductances associated with the interfaces (a',α') and (b',β'). The total conductance is given by $1/G_{\rm tot}=1/g_a+1/g_b$. The two interfaces are thus in series which is because transport is mediated by the crossed Andreev reflection: a spin-up electron from the normal metal is transferred at site a', travels to site a, and is reflected as a spin-down hole at site b. The spin-down hole travels to site b' and is transferred in the normal metal at site β'. As a consequence of this transport process the two interfaces (a',α') and (b',β') are coupled in series.

D. Sequential tunneling through the *S*/DW/*S* junction

We consider the same model as in the preceding section but now the electrode on the right is superconducting (see Fig. 5). We show that the properties of the *S*/DW/*S* junction are similar to the properties of the *S*/DW/*N* junction. We suppose that a voltage V is applied on the left electrode and a voltage V' is applied on the right electrode. We consider a regime in which inelastic scattering in the ferromagnetic electrodes is strong enough so that the transport dwell time is much larger than the energy relaxation time (see Sec. IV A). Moreover, we suppose that inelastic scattering is strong enough so that there is no Josephson effect.

We consider that the ferromagnetic electrodes (a,a') and (b,b') are half-metal ferromagnets: $P_a=1$, $P_b=-1$. The total current is given by

$$\frac{I_{\rm tot}}{V'-V}=16\pi^2\rho_{a,\uparrow}\rho_{b,\downarrow}\frac{t_\alpha^2t_\beta^2t_{\alpha'}^2t_{\beta'}^2\langle\langle f_{\alpha,\beta}^2\rangle\rangle\langle\langle f_{\alpha',\beta'}^2\rangle\rangle}{t_\alpha^2t_\beta^2\langle\langle f_{\alpha,\beta}^2\rangle\rangle+t_{\alpha'}^2t_{\beta'}^2\langle\langle f_{\alpha',\beta'}^2\rangle\rangle}. \quad (48)$$

If we note $g=16\pi^2t_\alpha^2t_\beta^2\langle\langle f_{\alpha,\beta}^2\rangle\rangle$ and $g'=16\pi^2t_{\alpha'}^2t_{\beta'}^2\langle\langle f_{\alpha',\beta'}^2\rangle\rangle$, the conductances associated with the crossed Andreev reflection at the contacts with each of the two superconductors, we see that the total conductance is such that

$$\frac{1}{G_{\rm tot}}=\frac{1}{g}+\frac{1}{g'}, \quad (49)$$

which is the expected result since electron pairs travel in series through the two superconductors.

V. JOSEPHSON EFFECT IN THE *S*/DW/*S* JOSEPHSON JUNCTION

A. A two-channel model

Now we consider the *S*/DW/*S* junction in Fig. 5 in which the right electrode is superconducting. We suppose that $\tau_E\sim\tau_d\ll\tau_{sf}$ or $\tau_E<\tau_d\ll\tau_{sf}$ so that the two superconductors can be coupled coherently through the two ferromagnetic channels. We look for the condition under which a Josephson current can circulate across the junction. We suppose in this section that the two electrodes (a,a') and (b,b') are half-metal ferromagnets with antiparallel spin orientations. The case of a partial spin polarization and noncollinear spin orientations will be discussed in Sec. V B.

The Nambu representation of the hopping matrix elements is given by

$$\hat{t}_{\alpha,a}=\begin{bmatrix}t_\alpha e^{-i(\varphi-\chi)/4} & 0\\ 0 & -t_\alpha e^{i(\varphi-\chi)/4}\end{bmatrix}, \quad (50)$$

$$\hat{t}_{\beta,b}=\begin{bmatrix}t_\beta e^{-i(\varphi+\chi)/4} & 0\\ 0 & -t_\beta e^{i(\varphi+\chi)/4}\end{bmatrix}, \quad (51)$$

$$\hat{t}_{a',\alpha'}=\begin{bmatrix}t_{\alpha'} e^{-i(\varphi-\chi)/4} & 0\\ 0 & -t_{\alpha'} e^{i(\varphi-\chi)/4}\end{bmatrix}, \quad (52)$$

$$\hat{t}_{b',\beta'}=\begin{bmatrix}t_{\beta'} e^{-i(\varphi+\chi)/4} & 0\\ 0 & -t_{\beta'} e^{i(\varphi+\chi)/4}\end{bmatrix}, \quad (53)$$

where φ is the difference between the superconducting phases in the right and left electrode and χ is the magnetic flux through the loop. We have the relations $\hat{t}_{a,\alpha}=(\hat{t}_{\alpha,a})^*$, $\hat{t}_{b,\beta}=(\hat{t}_{\beta,b})^*$, $\hat{t}_{\alpha',a'}=(\hat{t}_{a',\alpha'})^*$, and $\hat{t}_{\beta',b'}=(\hat{t}_{b',\beta'})^*$. The equilibrium current flowing from site α to site a is given by

$$I_{\alpha,a}=\frac{e}{h}\int d\omega\, n_F(\omega){\rm Tr}\{\hat{\sigma}^z[\hat{t}_{\alpha,a}(\hat{G}_{a,\alpha}^A-\hat{G}_{a,\alpha}^R) -\hat{t}_{a,\alpha}(\hat{G}_{\alpha,a}^A-\hat{G}_{\alpha,a}^R)]\}. \quad (54)$$

The Green's functions are 2×2 matrices since we do not discuss noncollinear magnetizations for the moment.

We deduce from Eq. (54) that to order t^4 the spin-up current through electrode (a,a') is given by

$$I^{(\uparrow)}_{\alpha,a}=-2i\frac{e}{h}t_\alpha t_\beta t_{\alpha'}t_{\beta'}\sin\varphi\int_0^{+\infty}d\omega\, f_{\alpha,\beta}(\omega)f_{\alpha',\beta'}(\omega)\times\left\{\frac{g^{A,11}_{a,a'}g^{A,22}_{b,b'}}{\mathrm{Det}[\check{I}-\check{K}^A]}-\frac{g^{R,11}_{a,a'}g^{R,22}_{b,b'}}{\mathrm{Det}[\check{I}-\check{K}^R]}\right\}, \tag{55}$$

where $\check{K}^{A,R}$ is the 4×4 matrix involved in the Dyson equation $[\check{I}-\check{K}^{A,R}]\check{G}^{A,R}=\check{g}^{A,R}$:

$$\begin{bmatrix} 1-K^{1,1}_{a,a} & -K^{2,1}_{b,a} & -K^{1,1}_{a',a} & -K^{2,1}_{b',a} \\ -K^{1,2}_{a,b} & 1-K^{2,2}_{b,b} & -K^{1,2}_{a',b} & -K^{2,2}_{b',b} \\ -K^{1,1}_{a,a'} & -K^{2,1}_{b,a'} & 1-K^{1,1}_{a',a'} & -K^{2,1}_{b',a'} \\ -K^{1,2}_{a,b'} & -K^{2,2}_{b,b'} & -K^{1,2}_{a',b'} & 1-K^{2,2}_{b',b'} \end{bmatrix}\begin{bmatrix} G^{1,1}_{a,a} \\ G^{1,2}_{a,b} \\ G^{1,1}_{a,a'} \\ G^{1,2}_{a,b'} \end{bmatrix}=\begin{bmatrix} g^{1,1}_{a,a} \\ 0 \\ g^{1,1}_{a,a'} \\ 0 \end{bmatrix}, \tag{56}$$

where we used the notation $K^{1,1}_{a,a}=t^{1,1}_{a,\alpha}g_{\alpha,\alpha}t^{1,1}_{\alpha,a}g^{1,1}_{a,a}$, $K^{2,1}_{b,a}=t^{2,2}_{b,\beta}f_{\beta,\alpha}t^{1,1}_{\alpha,a}g^{1,1}_{a,a}$, etc. The role of disorder can be included in a straightforward fashion. Since the spin-up and spin-down electrons of the Cooper pair propagate in different electrodes we should replace $g^{A,1,1}_{a,a'}$ and $g^{A,2,2}_{b,b'}$ by their averages over disorder, which decay exponentially with distance over a length scale equal to the elastic mean free path.[54] We conclude that a Josephson current cannot be observed under usual experimental conditions since the size of the ferromagnetic region is usually much larger than the elastic mean free path. The opposite limit of small disorder is considered in Appendix D.

B. Multichannel effects

1. Transport formula

We consider in this section the multichannel S/DW/S junction on Fig. 6 in which the ferromagnetic metal is multiply connected to the superconductors. The local magnetization makes an angle $\theta(z)$ with the z axis. The situation with a uniform θ corresponds to the multichannel π junction.

The supercurrent is given by

$$I_S=\frac{1}{2}\frac{e}{h}\int_0^{+\infty}d\omega\sum_n \mathrm{Tr}\{\hat{\sigma}^z[\hat{t}_{\alpha_n,a_n}(\hat{G}^A_{a_n,\alpha_n}-\hat{G}^R_{a_n,\alpha_n})-\hat{t}_{a_n,\alpha_n}(\hat{G}^A_{\alpha_n,a_n}-\hat{G}^R_{\alpha_n,a_n})]\}, \tag{57}$$

where the Green's functions are 4×4 matrices. The supercurrent to order $t^2_\alpha t^2_\beta$ can be written as

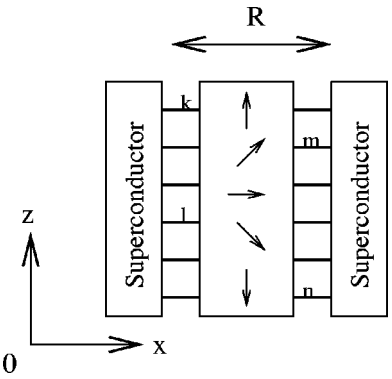

FIG. 6. Schematic representation of the Josephson junction containing a domain wall with a rotating magnetization. The x and z axes are shown in the figure. The y axis is perpendicular to the figure.

$$I_S=-2i\frac{e}{h}t^2_\alpha t^2_\beta\sin\varphi\int_0^{+\infty}d\omega\sum_{k,l,m,n}f_{\alpha_m,\alpha_n}f_{\beta_k,\beta_l}\times\left\{\left[\frac{g^{2,2,A}_{a_m,b_k}g^{1,1,A}_{a_n,b_l}}{\mathrm{Det}[\check{I}-\check{K}^A]}-\frac{g^{2,2,R}_{a_m,b_k}g^{1,1,R}_{a_n,b_l}}{\mathrm{Det}[\check{I}-\check{K}^R]}\right]+\left[\frac{g^{4,4,A}_{a_m,b_k}g^{3,3,A}_{a_n,b_l}}{\mathrm{Det}[\check{I}-\check{K}^A]}-\frac{g^{4,4,R}_{a_m,b_k}g^{3,3,R}_{a_n,b_l}}{\mathrm{Det}[\check{I}-\check{K}^R]}\right]+2\left[\frac{g^{2,4,A}_{a_m,b_k}g^{1,3,A}_{a_n,b_l}}{\mathrm{Det}[\check{I}-\check{K}^A]}-\frac{g^{2,4,R}_{a_m,b_k}g^{1,3,R}_{a_n,b_l}}{\mathrm{Det}[\check{I}-\check{K}^R]}\right]\right\}, \tag{58}$$

where $g^{i,i}_{a_k,b_m}$ is ith Nambu component of the propagator connecting the two ends of the ferromagnetic metal at sites a_k and b_m. The first two terms in the right-hand side (r.h.s.) of Eq. (58) correspond to a propagation without spin flip in the ferromagnetic region, whereas the last term corresponds to a propagation with spin flip. We deduce from Eq. (58) the same conclusions as in the two-channel model. Namely an average Josephson current can circulate only if the size of the ferromagnetic region is smaller than the elastic mean free path in the ferromagnetic metal, a condition that is not usually realized in experiments.

2. Limit of small disorder

To obtain the supercurrent in the ballistic limit we replace the propagators by their expressions and sum over all channels. The propagators of a ferromagnetic metal with a rotating magnetization are not known in general. This is why we discuss here only the situation where the width of the domain wall is vanishingly small and the ferromagnets are half-metal ferromagnets. In this case there is no spin precession in the ferromagnetic region but there exist trajectories parallel to the interface that we can take into account in our calculation. The supercurrent is given by

$$I_S=8\pi\frac{e}{h}L_y t^2_\alpha t^2_\beta\sin\varphi\left(\frac{ma_0^2}{\hbar^2}\right)^4 G(k_F), \tag{59}$$

with

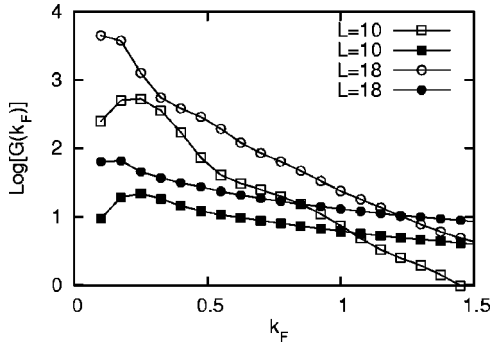

FIG. 7. Variation of $\log_{10}[G(k_F)]$ as a function of k_F. k_F is measured in units of $1/a_0$. We restrict the integration in Eq. (60) to $-L_z/2 \leqslant z_n,\ z_l < 0,\ 0 < z_m,\ z_k \leqslant L_z/2,\ -L_y/2 \leqslant y_n,\ y_l,\ y_m,\ y_k \leqslant L_y/2$ and we use $L = L_y = L_z$. The open symbols correspond to all trajectories in Eq. (60). The filled symbols correspond only to the trajectories perpendicular to the interface.

$$G(k_F) = \frac{1}{L_y}\int_{-\infty}^{0}\frac{dz_n}{a_0}\int_{-\infty}^{+\infty}\frac{dy_n}{a_0}\int_{-\infty}^{0}\frac{dz_l}{a_0}\int_{-\infty}^{+\infty}\frac{dy_l}{a_0} \times \int_{0}^{+\infty}\frac{dz_m}{a_0}\int_{-\infty}^{+\infty}\frac{dy_m}{a_0}\int_{0}^{+\infty}\frac{dz_k}{a_0}\int_{-\infty}^{+\infty}\frac{dy_k}{a_0} \quad (60)$$

$$\times \frac{a_0}{2\pi R_{\alpha_m,\alpha_n}}\frac{a_0}{2\pi R_{\beta_k,\beta_l}}\frac{a_0}{2\pi R_{a_m,b_k}}\frac{a_0}{2\pi R_{a_n,b_l}} \times \sin[k_F R_{\alpha_m,\alpha_n}]\sin[k_F R_{\beta_k,\beta_l}] \times \cos[k_F(R_{a_m,b_k} - R_{a_n,b_l})], \quad (61)$$

and with

$$R_{\alpha_m,\alpha_n} = \sqrt{(z_n - z_m)^2 + (y_m - y_n)^2}, \quad (62)$$

$$R_{\beta_k,\beta_l} = \sqrt{(z_k - z_l)^2 + (y_k - y_l)^2}, \quad (63)$$

$$R_{a_m,b_k} = \sqrt{R^2 + (z_m - z_k)^2 + (y_m - y_k)^2} \quad (64)$$

$$R_{a_n,b_l} = \sqrt{R^2 + (z_n - z_l)^2 + (y_n - y_l)^2}, \quad (65)$$

where R is the longitudinal dimension of the junction (see Fig. 6). We have shown on Fig. 7 the variation of $G(k_F)$ as a function of k_F. We see that strong finite size effects are present but still we can make a comparison between (i) a calculation in which all trajectories are taken into account and (ii) a calculation in which only the trajectories perpendicular to the interface are taken into account. We see that for small values of k_F (typically k_F smaller than $1/a_0$, where a_0 is the lattice parameter) the summation (i) is larger than (ii), whereas the opposite is true for larger values of k_F. This shows that trajectories parallel to the interface play a relevant role in the determination of the supercurrent.

VI. CONCLUSIONS

To conclude we have presented a detailed investigation of several mechanisms involved in transport across several junctions involving ferromagnetic domain walls (S/DW, S/DW/N, and S/DW/S junctions). The role of noncollinear magnetization was studied for the S/DW junctions. Using a spin⊗Nambu⊗Keldysh formalism we have derived the form of lowest-order transport formula valid for an arbitrary profile of magnetization. We find that the conductance is a scaling function of ξ_0/D, where ξ_0 is the zero-energy BCS correlation length and D is the width of the domain wall. Because of the proximity effect an exchange field can be induced in the superconductor. Neglecting the spatial variation of the exchange field, we have derived the transport formula and shown that there was no spin precession around the axis of the exchange field. We discussed the transport formula of the S/DW/N junction. We have shown that to lowest order only the processes taking place locally at each interface played a role. These processes are elastic cotunneling through the superconductor, crossed Andreev reflection, electron tunneling from the ferromagnet to the normal metal, and elastic cotunneling through the normal metal. We described the transport of Cooper pairs across the S/DW/N and S/DW/S junctions in a regime where transport is dominated by inelastic scattering but spin is conserved. With these assumptions the local distribution function within the domain wall is a Fermi distribution with a different spin-up and spin-down chemical potential. This model provides a detailed description of the sequential tunneling of Cooper pairs across the S/DW/N and S/DW/S junctions. We described the Josephson effect in a S/DW/S junction. Diffusion is usually strong in a ferromagnet and disorder is thus expected to play a relevant role. In particular the Josephson current decays exponentially with the longitudinal dimension of the junction. The characteristic length is equal to the mean free path in the ferromagnetic metal. This means that a Josephson current cannot be observed in usual conditions. Nevertheless there can exist a finite current due to a crossed Andreev reflection associated with elastic cotunneling in the ferromagnetic region.

ACKNOWLEDGMENTS

The authors acknowledge fruitful discussions with H. Courtois, D. Feinberg, M. Giroud, and B. Pannetier.

APPENDIX A: SPIN PRECESSION IN THE METALLIC CASE

In this appendix we consider the junction on Fig. 8 in which two ferromagnetic electrodes with noncollinear magnetizations are connected to a normal metal.[52,53] Our goal is to provide a comparison with the superconducting case presented in Sec. III C. We suppose that a magnetic field h is applied on the normal metal and that the only effect of the magnetic field is to generate Zeeman splitting. The crossed conductance $G_{a,b} = \partial I_a/\partial V_b$ associated with elastic cotunneling takes the form

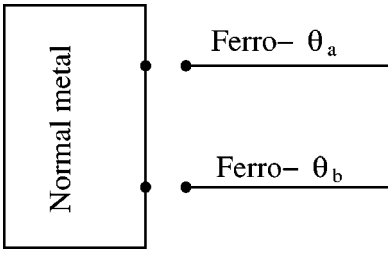

FIG. 8. The device considered in Appendix A. The electrode ending at site a is a ferromagnet with a magnetization pointing in the direction θ_a. The electrode ending at site b is a ferromagnet with a magnetization pointing in the direction θ_b.

$$G_{a,b}=8\pi^2 t_\alpha^2 t_\beta^2 \tilde{\rho}_a \tilde{\rho}_b \left(\frac{m a_0^2}{\hbar^2}\right)^2 \left(\frac{a_0}{2\pi R_{\alpha,\beta}}\right)^2 \times 1+P_a P_b \cos\theta_a \cos\theta_b + P_a P_b \sin\theta_a \sin\theta_b \times \cos\left\{[k_{F,\uparrow}-k_{F,\downarrow}]R_{\alpha,\beta}+eV_b\left[\frac{1}{v_{F,\uparrow}}-\frac{1}{v_{F,\downarrow}}\right]R_{\alpha,\beta}\right\}. \tag{A1}$$

Spin precession can have two origins: (i) the term $[k_{F,\uparrow}-k_{F,\downarrow}]R_{\alpha,\beta}$ describes oscillations of the conductance due to a mismatch in the Fermi wave vectors; (ii) the term $[1/v_{F,\uparrow}-1/v_{F,\downarrow}]R_{\alpha,\beta}$ describes oscillations in the conductance due to a mismatch in the Fermi velocities.

APPENDIX B: PERTURBATIVE TRANSPORT FORMULA OF THE TWO-CHANNEL *S*/DW/*N* JUNCTION

In this appendix we provide a derivation of the transport formula of the S/DW/N model represented in Fig. 5.

1. Transport at interface (a,α)

The current through each link of the network on Fig. 5 is given by the transport formula (4). The spin-up current through the link α-a is found to be

$$I_{a,\alpha}^{(\uparrow)}=-4\pi^2 t_\alpha^4 \tilde{\rho}_a^2 f_{\rm loc}^2[1-P_a^2][n_F(\omega-\mu_{a,\uparrow})-n_F(\omega+\mu_{a,\downarrow})] \tag{B1}$$

$$-4\pi^2 t_\alpha^2 t_\beta^2 \tilde{\rho}_a \tilde{\rho}_b g_{\alpha,\beta}^2[1+P_a][1+P_b][n_F(\omega-\mu_{a,\uparrow}) - n_F(\omega-\mu_{b,\uparrow})] \tag{B2}$$

$$-4\pi^2 t_\alpha^2 t_\beta^2 \tilde{\rho}_a \tilde{\rho}_b f_{\alpha,\beta}^2[1+P_a][1-P_b][n_F(\omega-\mu_{a,\uparrow}) - n_F(\omega+\mu_{b,\downarrow})] \tag{B3}$$

$$-4\pi^2 t_\alpha^2 t_{\alpha'}^2 \rho_{a,a'}^{\uparrow}\rho_{a,a'}^{\downarrow} f_{\rm loc}^2[n_F(\omega-\mu_{a,\uparrow}) - n_F(\omega+\mu_{a,\downarrow})] \tag{B4}$$

$$-4\pi^2 t_\alpha t_\beta t_{\alpha'} t_{\beta'} \rho_{a,a'}^{\uparrow}\rho_{b,b'}^{\uparrow} g_{\alpha,\beta} g_{\alpha',\beta'} \times[n_F(\omega-\mu_{a,\uparrow})-n_F(\omega-\mu_{b,\uparrow})] \tag{B5}$$

$$-4\pi^2 t_\alpha t_\beta t_{\alpha'} t_{\beta'} \rho_{a,a'}^{\uparrow}\rho_{b,b'}^{\downarrow} f_{\alpha,\beta} f_{\beta,\alpha} \times[n_F(\omega-\mu_{a,\uparrow})-n_F(\omega+\mu_{b,\downarrow})] \tag{B6}$$

$$-4\pi t_\alpha t_\beta t_{\alpha'} t_{\beta'}\, {\rm Im}[g_{a,a'}^{\uparrow R} g_{b,b'}^{\uparrow A}] g_{\alpha,\beta} g_{\alpha',\beta'} n_F(\omega-\mu'), \tag{B7}$$

where $\mu_{a,\uparrow}$ and $\mu_{a,\downarrow}$ are the spin-up and spin-down chemical potentials in electrode (a,a'), $\mu_{b,\uparrow}$ and $\mu_{b,\downarrow}$ are the spin-up and spin-down chemical potentials in electrode (b,b'), and μ' is the chemical potential in the normal metal. After phase averaging we obtain three contributions to the transport formula: local Andreev reflection given by term (38), elastic cotunneling through the superconductor given by term (39) and crossed Andreev reflection given by term (40).

2. Transport at interface (a',α')

The same calculation can be carried out at interface (a',α'). The transport formula is found to be

$$I_{a',\alpha'}^{(\uparrow)}=4\pi^2 t_{\alpha'}^2 t_{\beta'}^2 \tilde{\rho}_a \tilde{\rho}_b g_{\alpha',\beta'}^A g_{\alpha',\beta'}^R [1+P_a][1+P_b] n_F(\omega-\mu_{b,\uparrow}) - 8\pi^4 t_{\alpha'}^2 t_{\beta'}^2 \tilde{\rho}_a \tilde{\rho}_b \rho_{\alpha',\beta'}^2 [1+P_a][1+P_b] n_F(\omega-\mu')$$

$$-4\pi^2 t_{\alpha'}^2 \tilde{\rho}_a \rho' [1+P_a][n_F(\omega-\mu_{a,\uparrow})-n_F(\omega-\mu')] + 8\pi^4 t_{\alpha'}^4 (\tilde{\rho}_a)^2 (\rho')^2 [1+P_a]^2 [n_F(\omega-\mu_{a,\uparrow})-n_F(\omega-\mu')]$$

$$-8\pi^2 t_\alpha^2 t_{\alpha'}^2 \rho' g\, {\rm Re}[g_{a,a'}^{\uparrow}] \rho_{a,a'}^{\uparrow} n_F(\omega-\mu_{a,\uparrow}) + 2\pi^2 t_\alpha^2 t_{\alpha'}^2 (\rho')^2 (g_{a,a'}^{\uparrow R})^2 n_F(\omega-\mu') - 2i\pi t_\alpha^2 t_{\alpha'}^2 \rho' g (g_{a,a'}^{\uparrow A})^2$$

$$\times n_F(\omega-\mu') - 4\pi^2 t_\alpha t_\beta t_{\alpha'} t_{\beta'} g_{\alpha,\beta} \rho_{a,a'}^{\uparrow}\, {\rm Im}[g_{\alpha',\beta'}^A g_{b,b'}^{\uparrow A}] n_F(\omega-\mu_{a,\uparrow}) + 2i\pi t_\alpha t_\beta t_{\alpha'} t_{\beta'} g_{\alpha,\beta} \rho_{b,b'}^{\uparrow}$$

$$\times [g_{\alpha',\beta'}^A g_{a,a'}^{\uparrow R} + i\pi\rho' g_{a,a'}^{\uparrow A}] n_F(\omega-\mu_{b,\uparrow}) + 2i\pi t_\alpha t_\beta t_{\alpha'} t_{\beta'} g_{\alpha,\beta} \rho_{\alpha',\beta'} [g_{a,a'}^{\uparrow R} g_{b,b'}^{\uparrow R} - i\pi\tilde{\rho}_b (1+P_b) g_{a,a'}^{\uparrow A}]$$

$$\times n_F(\omega-\mu') - 4\pi^2 t_{\alpha'}^2 t_{\beta'}^2 \tilde{\rho}_a \tilde{\rho}_b\, {\rm Re}[(g_{\alpha',\beta'}^A)^2][1+P_a][1+P_b] n_F(\omega-\mu_{a,\uparrow}). \tag{B8}$$

After averaging over the phase variables we obtain the transport formula given by Eqs. (41)–(43) that contains only two processes: tunneling from site a' to site α' and elastic cotunneling from site b' to site a'.

APPENDIX C: TRANSPORT FORMULA OF THE SYMMETRIC TWO-CHANNEL *S*/DW/*N* AND *S*/DW/*S* JUNCTIONS

In this appendix we consider $S/\mathrm{DW}/N$ and $S/\mathrm{DW}/S$ junctions with two symmetric channels. With this model we confirm the results obtained in the main body of the article for the asymmetric junction with half-metal ferromagnets. We suppose that the two channels have an identical density of states, $\tilde{\rho}_a=\tilde{\rho}_b$, that the tunnel matrix elements are identical in the two channels, $t=t_\alpha=t_\beta$, $t'=t_{\alpha'}=t_{\beta'}$, and that the two channels have an opposite spin polarization, $P_a=P$ and $P_b=-P$. Then there exists a simple symmetry relation between the chemical potentials in the two ferromagnetic electrodes, $\mu_{a,\uparrow}=\mu_{b,\downarrow}$ and $\mu_{a,\downarrow}=\mu_{b,\uparrow}$.

1. The *S*/DW/*N* junction

In the limiting case $t\ll t'$ we have $\mu_{a,\uparrow}\simeq V'$. The transport formula is identical to the case where electrodes (a,a') and (b,b') are in equilibrium:

$$\frac{I_{\mathrm{tot}}}{V'}=32\pi^2t^4\tilde{\rho}^2(1-P^2)f_{\mathrm{loc}}^2+32\pi^2t^4\tilde{\rho}^2(1+P^2)\langle\langle f_{\alpha,\beta}^2\rangle\rangle. \tag{C1}$$

In the case of half-metal ferromagnets ($P=1$) only the term corresponding to the crossed Andreev reflection is nonzero, and Eq. (C1) is equivalent to Eq. (46).

In the limiting case $\rho_N t'\ll\rho_N t\ll 1$ and $t'\ll\rho_N t^2$ the current is the sum of a contribution due to the local Andreev reflection (AR) and a contribution due to the crossed Andreev reflection (CAR): $I_{\mathrm{tot}}=I_{\mathrm{AR}}+I_{\mathrm{CAR}}$, with

$$\frac{I_{\mathrm{AR}}}{V'}=\frac{32\pi^2(t')^2\tilde{\rho}\rho'(1-P^2)f_{\mathrm{loc}}^2(\langle\langle f_{\alpha,\beta}^2\rangle\rangle+\langle\langle g_{\alpha,\beta}^2\rangle\rangle)}{(1-P^2)[f_{\mathrm{loc}}^2\langle\langle g_{\alpha,\beta}^2\rangle\rangle+\langle\langle f_{\alpha,\beta}^2\rangle\rangle^2]+(1+P^2)\langle\langle f_{\alpha,\beta}^2\rangle\rangle[f_{\mathrm{loc}}^2+\langle\langle g_{\alpha,\beta}^2\rangle\rangle]}, \tag{C2}$$

$$\frac{I_{\mathrm{CAR}}}{V'}=\frac{16\pi^2(t')^2\overline{\rho\rho}'\langle\langle f_{\alpha,\beta}^2\rangle\rangle[(1+P^2)(\langle\langle f_{\alpha,\beta}^2\rangle\rangle+\langle\langle g_{\alpha,\beta}^2\rangle\rangle)+2P^2(f_{\mathrm{loc}}^2-\langle\langle f_{\alpha,\beta}^2\rangle\rangle)]}{(1-P^2)[f_{\mathrm{loc}}^2\langle\langle g_{\alpha,\beta}^2\rangle\rangle+\langle\langle f_{\alpha,\beta}^2\rangle\rangle^2]+(1+P^2)\langle\langle f_{\alpha,\beta}^2\rangle\rangle[f_{\mathrm{loc}}^2+\langle\langle g_{\alpha,\beta}^2\rangle\rangle]}. \tag{C3}$$

In the case of half-metal ferromagnets Eqs. (C2) and (C3) are equivalent to Eq. (47).

2. The *S*/DW/*S* junction

In the case of the $S/\mathrm{DW}/S$ junction the total current is the sum of the local Andreev reflection and crossed Andreev reflection terms:

$$\begin{aligned}\frac{I_{\mathrm{AR}}}{V'-V}=\frac{128\pi^2}{\mathcal{D}'}t^4(t')^4\tilde{\rho}^4f_{\mathrm{loc}}^2(1-P^2)\{&[t^4\langle\langle g_{\alpha,\beta}^2\rangle\rangle\\&+(t')^4\langle\langle g_{\alpha',\beta'}^2\rangle\rangle][(1-P^2)f_{\mathrm{loc}}^2+(1+P^2)\\&\times\langle\langle f_{\alpha,'\beta'}^2\rangle\rangle]+[t^4\langle\langle f_{\alpha,\beta}^2\rangle\rangle+(t')^4\langle\langle f_{\alpha',\beta'}^2\rangle\rangle]\\&\times[(1+P^2)f_{\mathrm{loc}}^2+(1-P^2)\langle\langle f_{\alpha',\beta'}^2\rangle\rangle]\},\end{aligned} \tag{C4}$$

$$\begin{aligned}\frac{I_{\mathrm{CAR}}}{V'-V}=\frac{128\pi^2}{\mathcal{D}'}t^4(t')^4\tilde{\rho}^4\langle\langle f_{\alpha,\beta}^2\rangle\rangle(1+P^2)\{&[t^4\langle\langle g_{\alpha,\beta}^2\rangle\rangle\\&+(t')^4\langle\langle g_{\alpha',\beta'}^2\rangle\rangle][(1-P^2)f_{\mathrm{loc}}^2+(1+P^2)\\&\times\langle\langle f_{\alpha',\beta'}^2\rangle\rangle]+[t^4\langle\langle f_{\alpha,\beta}^2\rangle\rangle+(t')^4\langle\langle f_{\alpha',\beta'}^2\rangle\rangle]\\&\times[(1+P^2)f_{\mathrm{loc}}^2+(1-P^2)\langle\langle f_{\alpha',\beta'}^2\rangle\rangle]\},\end{aligned} \tag{C5}$$

with

$$\begin{aligned}\mathcal{D}'=4t^8\tilde{\rho}^2\{&(1-P^2)[f_{\mathrm{loc}}^2\langle\langle g_{\alpha,\beta}^2\rangle\rangle+\langle\langle f_{\alpha,\beta}^2\rangle\rangle^2]+(1+P^2)\\&\times[f_{\mathrm{loc}}^2\langle\langle f_{\alpha,\beta}^2\rangle\rangle+\langle\langle f_{\alpha,\beta}^2\rangle\rangle\langle\langle g_{\alpha,\beta}^2\rangle\rangle]\}+4(t')^8\tilde{\rho}^2\{(1\\&-P^2)[f_{\mathrm{loc}}^2\langle\langle g_{\alpha',\beta'}^2\rangle\rangle+\langle\langle f_{\alpha',\beta'}^2\rangle\rangle^2]+(1+P^2)\\&\times[f_{\mathrm{loc}}^2\langle\langle f_{\alpha',\beta'}^2\rangle\rangle^2+\langle\langle f_{\alpha',\beta'}^2\rangle\rangle\langle\langle g_{\alpha',\beta'}^2\rangle\rangle]\}\\&+4t^4(t')^4\tilde{\rho}^2\{(1-P^2)[f_{\mathrm{loc}}^2\langle\langle g_{\alpha,\beta}^2\rangle\rangle+f_{\mathrm{loc}}^2\langle\langle g_{\alpha',\beta'}^2\rangle\rangle\\&+2\langle\langle f_{\alpha,\beta}^2\rangle\rangle\langle\langle f_{\alpha',\beta'}^2\rangle\rangle]+(1+P^2)[f_{\mathrm{loc}}^2\langle\langle f_{\alpha,\beta}^2\rangle\rangle\\&+f_{\mathrm{loc}}^2\langle\langle f_{\alpha',\beta'}^2\rangle\rangle+\langle\langle f_{\alpha,\beta}^2\rangle\rangle\langle\langle g_{\alpha',\beta'}^2\rangle\rangle+\langle\langle f_{\alpha',\beta'}^2\rangle\rangle\\&\times\langle\langle g_{\alpha,\beta}^2\rangle\rangle]\}.\end{aligned} \tag{C6}$$

If the contacts with the two superconductors are identical, we have $t=t'$, $f_{\alpha,\beta}=f_{\alpha',\beta'}$, and $g_{\alpha,\beta}=g_{\alpha',\beta'}$ from which we deduce

$$\frac{1_{\mathrm{AR}}}{V'-V}=4\pi^2t^4\rho^2f_{\mathrm{loc}}^2(1-P^2), \tag{C7}$$

$$\frac{I_{\mathrm{CAR}}}{V'-V}=4\pi^2t^4\rho^2\langle\langle f_{\alpha,\beta}^2\rangle\rangle(1+P^2), \tag{C8}$$

where we used the notation $\tilde{\rho}=\rho/2$ for the spin-up or spin-down density of state in the ferromagnetic electrodes. Equations (C7) and (C8) in the limit $P=1$ are in agreement with Eq. (48) in the limit of a symmetric contact. In the symmetric case the conductance is thus equal to the conductance associated to a single superconductor divided by 2, in agreement with Eq. (49).

APPENDIX D: JOSEPHSON EFFECT IN A TWO-CHANNEL BALLISTIC *S*/DW/*S* JUNCTION

In this appendix we describe the Josephson effect with a ballistic propagation in the ferromagnetic electrodes. In the limit of a long junction $R \gg a_0$ the matrix $\check{I}-\check{K}^{A,R}$ given by Eq. (56) is block-diagonal because the Andreev bound states do not couple the two superconductors. There exist two bound states associated with the interfaces (α,a) and (β,b) and two bound states associated with the interfaces (α',a') and (β',b'). The secular equation for the bound states existing at the interfaces (α,a) and (β,b) takes the form

$$1+i\pi^2\rho_F\rho_N(t_\alpha^2+t_\beta^2)\frac{\omega_0}{\sqrt{\Delta^2-\omega_0^2}} + (\pi^2\rho_F\rho_N)^2 t_\alpha^2 t_\beta^2 \frac{z^2\Delta^2-\omega_0^2}{\Delta^2-\omega_0^2}=0, \qquad \text{(D1)}$$

where ρ_N and ρ_F are the density of states in the superconductor and in the half-ferromagnetic electrodes, and where we used the notation $z=\sin[k_F R]/(k_F R)$. In the case $t=t_\alpha=t_\beta$ and in the tunnel limit $\pi t^2\rho_N\rho_F \ll 1$ the solution of Eq. (D1) takes the form

$$\omega_0^2=\Delta^2[1+(\pi^2 t^2\rho_N\rho_F)^2(1\pm z)^2]. \qquad \text{(D2)}$$

The supercurrent is easily deduced from Eq. (55):

$$I_S=\frac{16\pi^9}{(a_0k_F^{\uparrow})^2(a_0k_F)^2}\frac{e}{h}\Delta t^4\rho_N^2\rho_F^2(1+P)^2\frac{a_0}{2\pi R_{\alpha,\beta}}\frac{a_0}{2\pi R_{\alpha',\beta'}} \times\frac{a_0}{2\pi R_{a,\alpha'}}\frac{a_0}{2\pi R_{b,b'}}\sin[k_F R_{\alpha,\beta}]\sin[k_F R_{\alpha',\beta'}] \qquad \text{(D3)}$$

$$\times\exp\left\{-\left(\frac{R_{a,a'}+R_{b,b'}}{l_\phi}\right)\right\} f(z,z')\cos\alpha\sin\varphi, \qquad \text{(D4)}$$

where α is defined by

$$\alpha=k_F^{\uparrow}(R_{a,\alpha'}-R_{b,b'})+\frac{\Delta}{v_F^{\uparrow}}(R_{a,\alpha'}+R_{b,b'}), \qquad \text{(D5)}$$

and where $f(z,z')$ is a geometrical prefactor of order unity.

[1] M. S. Choi, C. Bruder, and D. Loss, Phys. Rev. B **62**, 13 569 (2000); P. Recher, E. V. Sukhorukov, and D. Loss, *ibid.* **63**, 165314 (2001).

[2] O. Sauret, D. Feinberg, and T. Martin, Eur. Phys. J. B **32**, 545 (2003).

[3] G. Deutscher and D. Feinberg, Appl. Phys. Lett. **76**, 487 (2000).

[4] G. Falci, D. Feinberg, and F. W. J. Hekking, Europhys. Lett. **54**, 255 (2001).

[5] R. Mélin, J. Phys.: Condens. Matter **13**, 6445 (2001); R. Mélin, in Proceedings of the XXXVIth Rencontres de Moriond, edited by T. Martin and G. Montambaux (EDP Sciences, 2001).

[6] R. Mélin and D. Feinberg, Eur. Phys. J. B **26**, 101 (2002).

[7] G. B. Lesovik, T. Martin, and G. Blatter, Eur. Phys. J. B **24**, 287 (2001); N. M. Chtchelkatchev, G. Blatter, G. B. Lesovik, and T. Martin, Phys. Rev. B **66**, 161320(R) (2002); V. Bouchiat, N. Chtchelkatchev, D. Feinberg, G. B. Lesovik, T. Martin, and J. Torres, cond-mat/0206005 (unpublished).

[8] P. Fulde and A. Ferrel, Phys. Rev. **135**, A550 (1964).

[9] A. Larkin and Y. Ovchinnikov, Zh. Eksp. Teor. Fiz 47, 1136 (1964) [Sov. Phys. JETP **20**, 762 (1965)].

[10] M. A. Clogston, Phys. Rev. Lett. **9**, 266 (1962).

[11] E. A. Demler, G. B. Arnold, and M. R. Beasley, Phys. Rev. B **55**, 15 174 (1997).

[12] A. I. Buzdin, L. N. Bulaevskii, and S. V. Panyukov, Pis'ma Zh. Eksp. Teor. Fiz. **35**, 147 (1982) [JETP Lett. **35**, 178 (1982)]; A. Buzdin, B. Bujicic, and M. Yu. Kupriyanov, Zh. Eksp. Teor. Fiz. **101**, 231 (1992) [Sov. Phys. JETP **74**, 124 (1992)].

[13] V. V. Ryazanov, V. A. Oboznov, A. Yu. Rusanov, A. V. Veretennikov, A. A. Golubov, and J. Aarts, Phys. Rev. Lett. **86**, 2427 (2001).

[14] T. Kontos, M. Aprili, J. Lesueur, and X. Grison, Phys. Rev. Lett. **86**, 304 (2001).

[15] M. Zareyan, W. Belzig, and Yu. V. Nazarov, Phys. Rev. Lett. **86**, 308 (2001).

[16] P. G. de Gennes, Phys. Lett. **23**, 10 (1966).

[17] I. Baladié, A. Buzdin, N. Ryzhanova, and A. Vedyayev, Phys. Rev. B **63**, 054518 (2001); I. Baladié and A. Buzdin, Phys. Rev. B **67**, 014523 (2003).

[18] V. Apinyan and R. Mélin, Eur. Phys. J. B **25**, 373 (2002).

[19] H. Jirari, R. Mélin, and N. Stefanakis, Eur. Phys. J. B **31**, 125 (2003).

[20] A. I. Buzdin and M. Yu. Kupriyanov, Pis'ma Zh. Eksp. Teor. Fiz. **52**, 1089 (1990) [JETP Lett. **52**, 487 (1990)]; A. I. Buzdin, M. Yu. Kupriyanov, and B. Vujicic, Physica C **185–189**, 2025 (1991).

[21] J. S. Jiang, D. Davidović, D. H. Reich, and C. L. Chien, Phys. Rev. Lett. **74**, 314 (1995).

[22] C. L. Chien, J. S. Jiang, J. Q. Xiao, D. Davidović, and D. H. Reich, J. Appl. Phys. **81**, 5358 (1997).

[23] L. V. Mercaldo, C. Attanasio, C. Coccorese, L. Maritato, S. L. Prischepa, and M. Salvato, Phys. Rev. B **53**, 14 040 (1996).

[24] J. S. Jiang, D. Davidović, D. H. Reich, and C. L. Chien, Phys. Rev. B **54**, 6119 (1996).

[25] Th. Muhge, N. N. Garif'yanov, Yu. V. Goryunov, G. G. Khaliullin, L. R. Tagirov, K. Westerholt, I. A. Garifullin, and H. Zabel, Phys. Rev. Lett. **77**, 1857 (1996); Th. Muhge, K. Westerholt, H. Zabel, N. N. Garif'yanov, Yu. V. Goryunov, I. A. Garifullin, and G. G. Khaliullin, Phys. Rev. B **55**, 8945 (1997).

[26] M. D. Lawrence and N. Giordano, J. Phys.: Condens. Matter **39**, L563 (1996).

[27] V. A. Vas'ko, V. A. Larkin, P. A. Kraus, K. R. Nikolaev, D. E. Grupp, C. A. Nordman, and A. M. Goldman, Phys. Rev. Lett. **78**, 1134 (1997).

[28] M. Giroud, H. Courtois, K. Hasselbach, D. Mailly, and B. Pannetier, Phys. Rev. **58**, R11 872 (1998).

[29] V. T. Petrashov, I. A. Sosnon, I. Cox, A. Parsons, and C. Troadec, Phys. Rev. Lett. **83**, 3281 (1999).
[30] A. T. Filip, B. H. Hoving, F. J. Jedema, B. J. van Wees, B. Dutta, and S. Borghs, Phys. Rev. B **62**, 9996 (2000).
[31] M. Giroud, K. Hasselbach, H. Courtois, D. Mailly, and B. Pannetier, Eur. Phys. J. B **31**, 103 (2003).
[32] M. J. M. de Jong and C. W. J. Beenakker, Phys. Rev. Lett. **74**, 1657 (1995).
[33] R. J. Soulen *et al.*, Science **282**, 85 (1998).
[34] S. K. Upadhyay, A. Palanisami, R. N. Louie, and R. Buhrman, Phys. Rev. Lett. **81**, 3247 (1998).
[35] F. S. Bergeret, A. F. Volkov, and K. B. Efetov, Phys. Rev. Lett. **18**, 4096 (2001).
[36] A. Kadigrobov, R. I. Shekhter, and M. Jonson, Europhys. Lett. **54**, 394 (2001).
[37] N. M. Chtchelkatchev and I. Burmistrov, Phys. Rev. B **68**, 140501(R) (2003).
[38] M. V. Feigel'man, A. I. Larkin, and M. A. Skvortsov, Phys. Rev. B **61**, 12 361 (2000).
[39] D. Huertas-Hernando, Yu. V. Nazarov, and W. Belzig, Phys. Rev. Lett. **88**, 047003 (2003).
[40] Z. Y. Zeng, B. Li, and F. Claro, cond-mat/0301264 (unpublished).
[41] T. Valet and A. Fert, Phys. Rev. B **48**, 7099 (1993); J. Magn. Magn. Mater. **121**, 378 (1993); A. Fert, T. Valet, and J. Barnas, J. Appl. Phys. **75**, 6693 (1994); A. Fert, J. L. Duvail, and T. Valet, Phys. Rev. B **52**, 6513 (1995).
[42] M. A. M. Gijs and G. Bauer, Adv. Phys. **46**, 285 (1997).
[43] R. Mélin and D. Denaro, Eur. Phys. J. B **18**, 149 (2000).
[44] S. Kasai, T. Niiyama, E. Saitoh, and H. Miyajima, Appl. Phys. Lett. **81**, 316 (2002).
[45] P. M. Tedrow and R. Meservey, Phys. Rev. Lett. **26**, 192 (1971); P. M. Tedrow and R. Meservey, Phys. Rev. B **7**, 318 (1973); R. Meservey and P. M. Tedrow, Phys. Rep. **238**, 173 (1994).
[46] G. Deutscher and F. Meunier, Phys. Rev. Lett. **22**, 395 (1969).
[47] J. J. Hauser, Phys. Rev. Lett. **23**, 374 (1969).
[48] Y. Tserkovnyak and A. Brataas, Phys. Rev. B **65**, 094517 (2002).
[49] J. C. Cuevas, A. Martin-Rodero, and A. Levy Yeyati, Phys. Rev. B **54**, 7366 (1996).
[50] A. Martin-Rodero, F. J. Garcia-Vidal, and A. Levy Yeyati, Phys. Rev. Lett. **72**, 554 (1994).
[51] A. Levy Yeyati, A. Martin-Rodero, and F. J. Garcia-Vidal, Phys. Rev. B **51**, 3743 (1995).
[52] D. Huertas Hernando, Yu. V. Nazarov, A. Brataas, and G. E. W. Bauer, Phys. Rev. B **62**, 5700 (2000).
[53] F. J. Jedema, A. T. Filip, and B. J. van Wees, Nature (London) **410**, 345 (2001); F. J. Jedema, H. B. Heersche, A. T. Filip, J. J. A. Baselmans, and B. J. van Wees, Nature (London) **416**, 713 (2002).
[54] A. A. Abrikosov, L. P. Gorkoy, and I. E. Dzyaloshinski, *Methods of Quantum Field Theory in Statistical Physics* (Dover, New York, 1963).